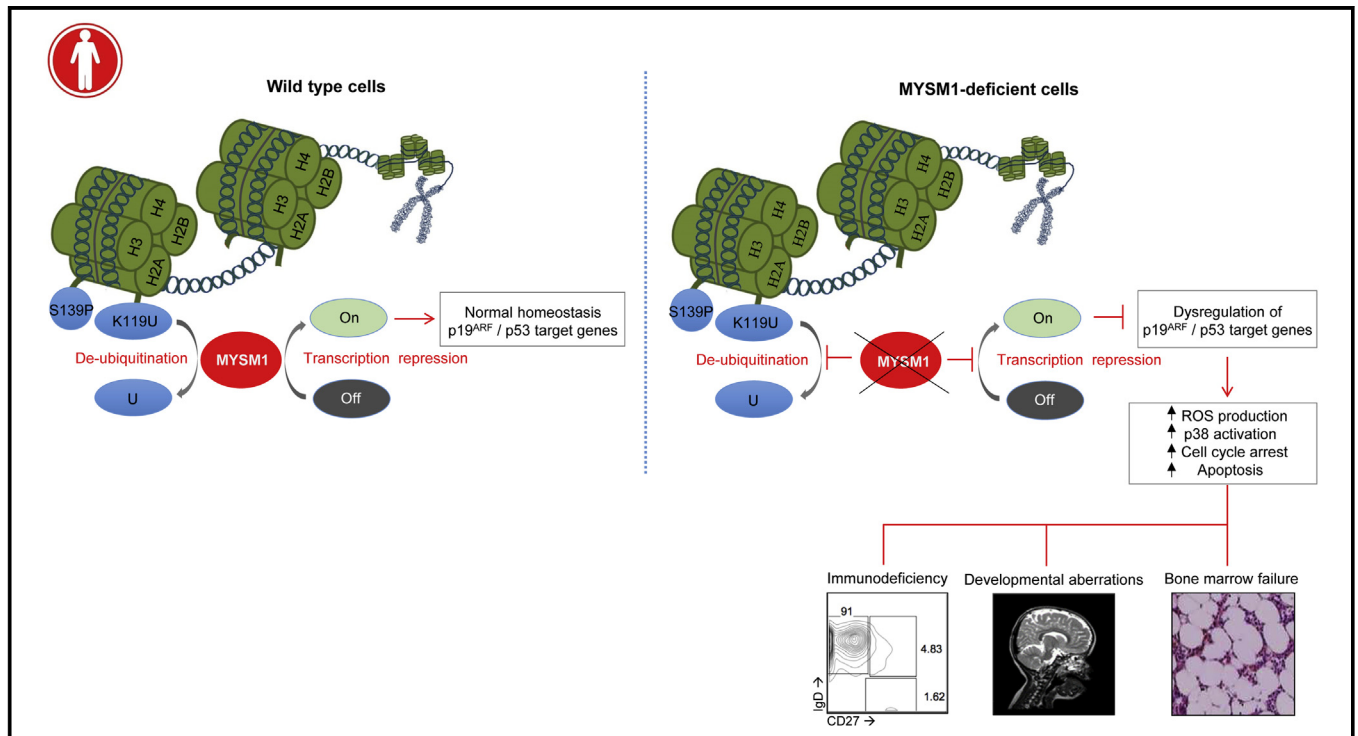


# Myb-like, SWIRM, and MPN domains 1 (MYSM1) deficiency: Genotoxic stress-associated bone marrow failure and developmental aberrations



Ehsan Bahrami, MSc,<sup>a</sup> Maximilian Witzel, MD,<sup>a</sup> Tomas Racek, PhD,<sup>a</sup> Jacek Puchaika, PhD,<sup>a,†</sup> Sebastian Hollizeck, MSc,<sup>a</sup> Naschla Greif-Kohistani, MD,<sup>a</sup> Daniel Kotlarz, MD, PhD,<sup>a</sup> Hans-Peter Horny, MD,<sup>b</sup> Regina Feederle, PhD,<sup>c</sup> Heinrich Schmidt, MD,<sup>a</sup> Roya Sherkat, MD,<sup>d</sup> Doris Steinemann, PhD,<sup>e</sup> Gudrun Göhring, MD,<sup>e</sup> Brigitte Schlegelbeger, MD,<sup>e</sup> Michael H. Albert, MD,<sup>a</sup> Waleed Al-Herz, MD,<sup>f</sup> and Christoph Klein, MD, PhD<sup>a</sup> *Munich and Hannover, Germany, Isfahan, Iran, and Kuwait City, Kuwait*

## GRAPHICAL ABSTRACT



**Background:** Myb-like, SWIRM, and MPN domains 1 (MYSM1) is a transcriptional regulator mediating histone deubiquitination. Its role in human immunity and hematopoiesis is poorly understood.

**Objectives:** We sought to investigate the clinical, cellular, and molecular features in 2 siblings presenting with progressive bone marrow failure (BMF), immunodeficiency, and developmental aberrations.

From <sup>a</sup>the Department of Pediatrics, Dr. von Hauner Children's Hospital, and <sup>b</sup>the Institute for Pathology, Faculty of Medicine, Ludwig-Maximilians-Universität, Munich; <sup>c</sup>Helmholtz Zentrum München. German Research Center for Environmental Health, Core Facility Monoclonal Antibody Development, Munich; <sup>d</sup>the Acquired Immunodeficiency Research Center, Isfahan University of Medical Sciences; <sup>e</sup>the Institute of Human Genetics, Hannover Medical School, Hannover; and <sup>f</sup>the Department of Pediatrics, Faculty of Medicine, Kuwait University, and Department of Pediatrics, Al-Sabah Hospital, Kuwait City.

<sup>†</sup>Deceased.

Supported by grants from the BMBF (German PID-NET, #01GM0894), the Leona M. and Harry B. Helmsley Charitable Trust (#2015PG-IBD008), the German Research Society (Gottfried Wilhelm Leibniz Program [#KL 877/11-1], SFB 1054 [#SFB 1054/1 A05]), German Research Foundation (DFG) through the excellence cluster REBIRTH (DFG #EXC 62), the European Research Council (ERC, Advanced Grant Explore [#268608-EXPLORE]), Reinhard-Frank Stiftung, the Else Kröner-Fresenius-

Stiftung (#2013\_Kolleg.18), DZIF/EKFS (#TTU 07.801), and the Care-for-Rare Foundation (#C4R/PrNr.140042).

Disclosure of potential conflict of interest: The authors declare that they have no relevant conflicts of interest.

Received for publication April 13, 2016; revised September 22, 2016; accepted for publication October 17, 2016.

Available online January 21, 2017.

Corresponding author: Christoph Klein, MD, PhD, Dr. von Hauner Children's Hospital, Lindwurmstrasse 2a, D-80337 München, Germany. E-mail: [christoph.klein@med.uni-muenchen.de](mailto:christoph.klein@med.uni-muenchen.de).

The CrossMark symbol notifies online readers when updates have been made to the article such as errata or minor corrections

0091-6749/\$36.00

© 2017 American Academy of Allergy, Asthma & Immunology

<http://dx.doi.org/10.1016/j.jaci.2016.10.053>

**Methods:** We performed genome-wide homozygosity mapping, whole-exome and Sanger sequencing, immunophenotyping studies, and analysis of genotoxic stress responses. p38 activation, reactive oxygen species levels, rate of apoptosis and clonogenic survival, and growth in immune and nonimmune cells were assessed. The outcome of allogeneic hematopoietic stem cell transplantation (HSCT) was monitored.

**Results:** We report 2 patients with progressive BMF associated with myelodysplastic features, immunodeficiency affecting B cells and neutrophil granulocytes, and complex developmental aberrations, including mild skeletal anomalies, neurocognitive developmental delay, and cataracts. Whole-exome sequencing revealed a homozygous premature stop codon mutation in the gene encoding MYSM1. MYSM1-deficient cells are characterized by increased sensitivity to genotoxic stress associated with sustained induction of phosphorylated p38 protein, increased reactive oxygen species production, and decreased survival following UV light-induced DNA damage. Both patients were successfully treated with allogeneic HSCT with sustained reconstitution of hematopoietic defects.

**Conclusions:** Here we show that MYSM1 deficiency is associated with developmental aberrations, progressive BMF with myelodysplastic features, and increased susceptibility to genotoxic stress. HSCT represents a curative therapy for patients with MYSM1 deficiency. (J Allergy Clin Immunol 2017;140:1112-9.)

**Key words:** Immunodeficiency, stem cells, hematopoiesis, rare disease, transplantation

Inherited bone marrow failure (BMF) syndromes comprise a heterogeneous group of disorders associated with dysfunction of hematopoietic stem or progenitor cells. Genetic analysis of these rare diseases has provided important insight into the fundamental biological principles governing genomic integrity in stem cells, such as DNA repair, telomere maintenance, or ribosomal biogenesis.<sup>1</sup> Although the hierarchical control of hematopoiesis by transcription factors is well studied, the relevance of epigenetic regulation remains less well understood. Myb-like, SWIRM, and MPN domains 1 (MYSM1) has originally been identified in a search for transcriptional regulators and was found to mediate histone deubiquitination, specifically at position lysine 119 (K119) of histone 2A (H2A), a common chromatin modification associated with gene silencing.<sup>2</sup> Targeted deletion of murine Mym1 results in severe hematopoietic defects associated with an early block of B-cell development<sup>3</sup>; dysfunction of stem cell maintenance, self-renewal, and differentiation<sup>4</sup>; and natural killer (NK) cell defects.<sup>5</sup> In human subjects exome sequencing studies have revealed potentially disease-causing mutations in *MYSM1* in 2 families with BMF and immunodeficiencies.<sup>6,7</sup> Here we study 2 patients with MYSM1 deficiency, including genetic reconstitution data and cellular studies illustrating decreased genotoxic stress resistance in patients with this rare genetic disorder.

## METHODS

### Patient information and study approval

Patients were referred to the Department of Pediatrics, Al-Sabah Hospital, Kuwait, and the Dr. von Hauner Children's Hospital at Ludwig-Maximilians-Universität Munich, Germany. Informed consent was obtained according to

#### Abbreviations used

BMF:	Bone marrow failure
EBV-LCL:	Epstein-Barr virus transformed B lymphoblastoid cell line
H2A:	Histone 2A
γ-H2AX:	Phospho-histone H2AX
HD:	Healthy donor
HSCT:	Hematopoietic stem cell transplantation
MAPK:	Mitogen-activated protein kinase
MYSM1:	Myb-Like, SWIRM, and MPN domains 1
RFP:	Red fluorescent protein

current ethical and legal guidelines. This study was conducted in accordance with the Declaration of Helsinki and was approved by the institutional review board of the Ludwig-Maximilians-Universität Munich.

### Next-generation sequencing and genetic analysis

Next-generation sequencing was performed, as previously described.<sup>8</sup> Briefly, genomic DNA isolated from whole blood of both patients and their parents were first analyzed with the Affymetrix Genome-wide Human SNP array 6.0 (GEO Platform GPL6801), according to the manufacturer's instructions (Affymetrix, Santa Clara, Calif). Remaining DNA has been used for generation of whole-exome libraries using the SureSelect XT Human All Exon V4 + UTRs kit (Agilent Technologies, Santa Clara, Calif). Barcoded libraries were sequenced with the SOLiD 5500 XL next-generation sequencing platform (Life Technologies, Grand Island, NY) to an average coverage depth of 80. Bioinformatic analysis and subsequent filtering of called variants led to identification of a potentially causative homozygous mutation (see [Table E1](#) in this article's Online Repository at [www.jacionline.org](http://www.jacionline.org)). All relevant variants were confirmed by using Sanger sequencing.

### Cell culture

Epstein-Barr virus transformed B lymphoblastoid cell lines (EBV-LCLs) were generated by infecting freshly isolated PBMCs with B95-8 cell supernatant in the presence of cyclosporine and maintained in RPMI 1640 medium supplemented with 10% heat-inactivated FBS, 1% penicillin/streptomycin, 1% HEPES, and 2 mmol/L L-glutamine at 37°C in the presence of 5% CO<sub>2</sub>. Fibroblasts were derived from skin or foreskin biopsy specimens, with continuous cultivation in Dulbecco modified Eagle medium and supplementation with 10% heat-inactivated FBS, 1% penicillin/streptomycin, and 2 mmol/L L-glutamine at 37°C in a 5% CO<sub>2</sub> atmosphere.

Further clinical data and methods are provided in the [Methods](#) section in this article's Online Repository at [www.jacionline.org](http://www.jacionline.org).

## RESULTS

### Clinical phenotype

We studied 2 siblings of a consanguineous Arab pedigree ([Fig 1, A](#)) with early-onset progressive BMF and myelodysplastic features.

Patient IV-1 was born prematurely and presented with severe anemia (hemoglobin, 3 g/dL) at birth, requiring immediate red blood cell transfusion. In her first 2 years of life, she was treated for recurrent upper respiratory tract infections. During one episode of severe infection, she was hospitalized, treated with intravenous antibiotics, and maintained on co-trimoxazole prophylaxis thereafter. She presented with BMF, short stature, and mild dysmorphic features, including thoracic asymmetry, a short left humerus, shortness of the metacarpal bone, dry skin, trigonocephaly, midface hypoplasia, gingiva hyperplasia, bilateral cataracts, and neurodevelopmental delay correlating

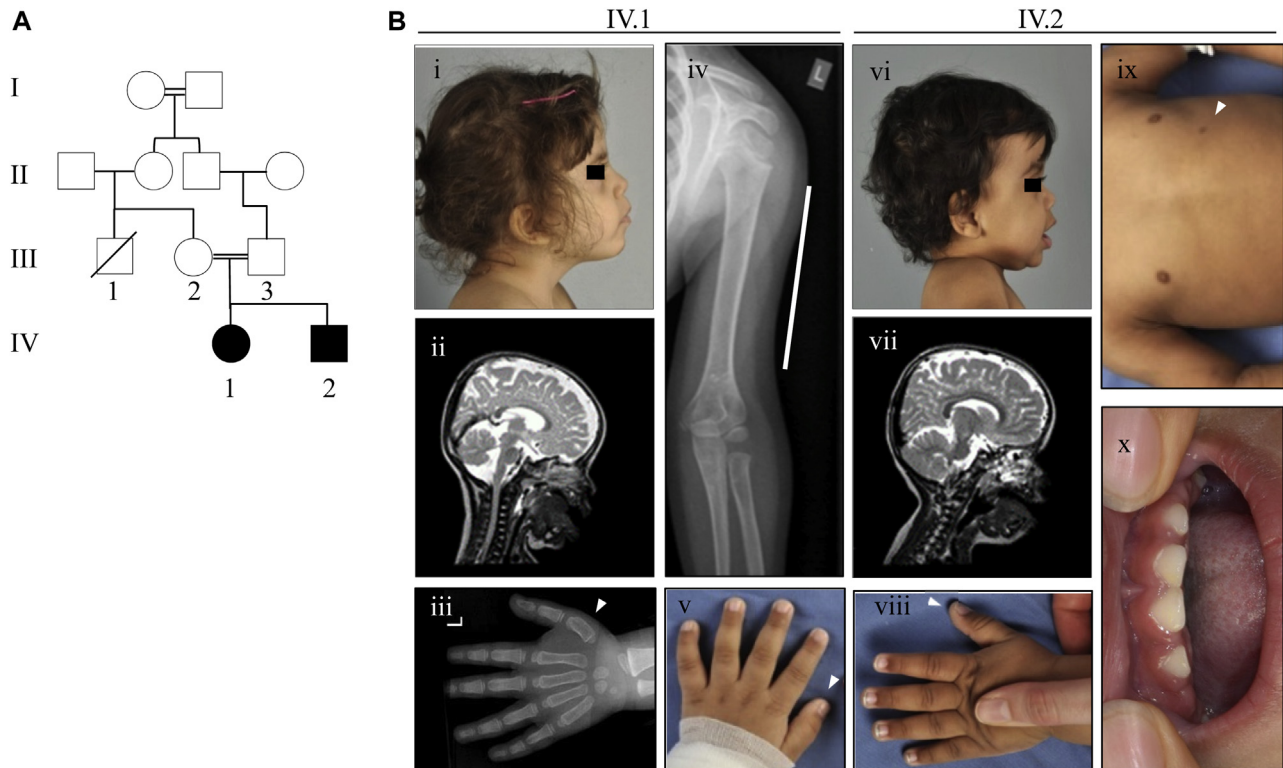


**FIG 1.** Pedigree, clinical, and immunologic phenotype of MYSM1-deficient patients. **A**, Pedigree of the family. **B**, Clinical phenotype of MYSM1-deficient patients with facial features, including midface hypoplasia, low-set ears, hypoplasia of the orbital floor, short neck (*i* and *vi*), magnetic resonance imaging correlates of increased liquor space and reduction of cerebral volume (*ii* and *vii*), short left humerus (*iv*, white line) and osteopenia (*iv*), brachymetacarpia/broad metacarpal bone D1 left (*iii*, arrowhead) and deep-set thumb (*v* and *viii*, arrowhead), accessory papilla of the breast (*ix*, arrowhead), and gingiva hyperplasia (*x*).

with reduced cerebral volume (Fig 1, B, *i-v*; Table I; and see Fig E1, *i-ii*).

Patient IV-2 was delivered preterm and had anemia (hemoglobin, 2 g/dL), as well as cardiac insufficiency requiring immediate cardiopulmonary resuscitation and transfusion. Until his second year of life, 2 episodes of upper airway infection were noted, but no further infections developed under co-trimoxazole prophylaxis. In our center he presented with BMF, short stature, and dysmorphic features, including rhizomelic shortening of the arms, short fingers, bilateral protrusions on collar bones, dry skin, eczema, accessory papilla of the breast, noncompaction cardiomyopathy, midface hypoplasia, gingiva hyperplasia, delayed dentition, and neurodevelopmental delay associated with reduced cerebral volume (Fig 1, B, *vi-x*; Table I; and see Fig E1, *iii-vi*).

Table I provides a comprehensive synopsis of known clinical feature courses in human MYSM1 deficiency. In both patients BMF manifested with transfusion-dependent anemia, mild thrombocytopenia, lymphopenia, and moderate-to-severe neutropenia (see Fig E3 in this article's Online Repository at [www.jacionline.org](http://www.jacionline.org)). Further investigations on sequential bone marrow biopsy specimens of the patients revealed hypocellularity, increased adipocytes (Fig 2, A, *i* and *v*), siderosis (see Fig E2, A, *i-iii*, in this article's Online Repository at [www.jacionline.org](http://www.jacionline.org)), and reduced numbers of megakaryocytes with pleomorphic aberrations (see Fig E2, A, *iv-vi*) and normal myeloperoxidase levels (see Fig E2, A, *vii-ix*).

Bone marrow cytology showed dysplastic findings of red and white blood cell precursors. Pseudo-Pelger-Huet anomaly, as well as dysplastic findings of erythroid lineages, including multinucleated erythroblasts, cytoplasmic bridges, and ectopic nuclear morphology of erythroblasts, was noted in both patients. No blast excess was noted (Fig 2, A, *ii-iv* and *vi-ix*, and see Fig E2, B, *i-iv*). We searched for mutations in genes frequently mutated in patients with myelodysplastic syndromes but could not identify any in the exome data set (see Table E2 in this article's Online Repository at [www.jacionline.org](http://www.jacionline.org)). Cytogenetic studies in myeloid precursor cells, as well as in mitomycin C-treated lymphoid cells, showed a normal karyogram according to chromosomal banding. Array-CGH data did not reveal a disease-causing copy number variation (data not shown).

Immunostaining of bone marrow samples was performed to further characterize early B- and T-cell development. Lymphoid TdT<sup>+</sup> progenitor and early B-cell progenitor (CD10<sup>+</sup> PAX<sup>+</sup>CD79a<sup>+</sup>) cell counts were markedly reduced, whereas CD3<sup>+</sup> cell counts were only mildly reduced (see Fig E2, A, *x-xxiv*). In line with these data, immunophenotypic analysis disclosed marked reduction of peripheral CD19<sup>+</sup>, marginal, and switched memory B-cell counts, which is consistent with B-cell deficiency. Further analysis of the B-cell compartment showed an increase in transitional (CD19<sup>+</sup>CD38<sup>Hi</sup>IgM<sup>Hi</sup>), activated CD19<sup>+</sup>CD21<sup>low</sup>CD38<sup>low</sup>, and plasmablast (CD19<sup>+</sup>CD38<sup>high</sup>IgM<sup>-</sup>) B cells (Fig 2, B).<sup>9,10</sup> T-cell immunophenotyping studies

**TABLE I.** Clinical phenotype of human MYSM1 deficiency

	Patient IV-1	Patient IV-2	Patient (Le Guen et al <sup>7</sup> )	Patient 1 (Alsultan et al <sup>6</sup> )	Patient 2 (Alsultan et al <sup>6</sup> )
Ethnicity	Arabic	Arabic	Turkish	Arabic	Arabic
Mutation	c.1168G>T;pE390*	c.1168G>T;pE390*	c.1967A>G, somatic reversion in peripheral blood (T, B, and NK cells and monocytes)	c.1168G>T;pE390*	c.1168G>T;pE390*
Infections/prophylaxis	Infant hospitalized for severe infections; consequently, co-trimoxazole, upper airway infections	Co-trimoxazole; free of infections	IVIG, co-trimoxazole; free of infections	NA	NA
Neonatology	Preterm 33rd gestational week, 1400 g, postpartum anemia Hb = 3 g/dL, RBC transfusion	Preterm 33rd gestational week 2120 g, postpartum anemia = Hb 2 g/dL, RBC transfusion, postpartum cardiopulmonary resuscitation	At term, 2620 g, Hb = 5 g/dL at birth, leukopenia respiratory stress because of choanal atresia	Normal growth parameters	ND
Growth	At 2 y, 4 mo*: Weight, 11 kg (percentile: 8.2%) Length, 81.5cm (percentile: 1.3%) Head, 47 cm (percentile, 30.9%)	At 3 mo*: Weight, 5.7 kg (percentile: 16.8%) Length, 53 cm (percentile: 0.0%) Head, 38 cm (percentile: 1.8%)	At birth*: Weight, 2.62 kg (percentile: 5.4%) Length, 47 cm (percentile: 6.4%) Head, 32 cm (percentile: 0.0%)	ND	ND
Hematology	IBMF, aregeneratory anemia tricytopenia, B-cell deficiency, dysplastic signs of granulopoiesis, erythropoiesis, megakaryopoiesis	IBMF, aregeneratory anemia tricytopenia, G6PDH deficiency B-cell deficiency, dysplastic signs of granulopoiesis, erythropoiesis, megakaryopoiesis	Aregenerative anemia BM: absence of erythroid precursors, normal granulopoiesis, B-cell deficiency	IBMF, pallor at 4 mo with Hb = 6 g/dL, transfusion dependent, until 9 mo, hypocellular bone marrow, thrombocytopenia 60,000/ $\mu$ L, spontaneous recovery of erythropoiesis	IBMF, pallor at 15 mo with Hb = 4.4 g/dL, transfusion dependent until 33 mo, pronounced erythropoiesis, reduced granulopoiesis, reduced megakaryopoiesis, dysplasia of erythroid precursors and megakaryocytes, negative HAM test result
Bones	Thoracic asymmetry, short left humerus, brachymetacarpia D1 left and broad metacarpia D1 left, osteopenia	Rhizomelic shortening of arms, short fingers	NA	NA	NA
Skin	Dry, itching skin, thin hair	Dry skin, eczema, leaf-like hypopigmentation on trunk, accessory papilla of breast	NA	NA	NA
Face	Trigonocephaly, hypoplasia of orbital floor, hypoplasia of zygomatic bones, midface hypoplasia, pointed chin, short neck, bilateral cataract	Midface hypoplasia, hypoplasia of orbital floor, short neck	NA	Facial dysmorpht†	NA
Heart	TI I°, dPmax 26 mm Hg, PFO with laminar LRS (incidental finding)	Cardiomegaly, left ventricle dilatation, reduced FS 16-20%, noncompaction cardiomyopathy	NA	NA	NA
Dental/mouth	Gingiva hyperplasia	Gingiva hyperplasia, delayed dentition	NA	NA	NA

(Continued)

TABLE I. (Continued)

	Patient IV-1	Patient IV-2	Patient (Le Guen et al <sup>7</sup> )	Patient 1 (Alsultan et al <sup>6</sup> )	Patient 2 (Alsultan et al <sup>6</sup> )
Neurology	Neuro developmental delay: increased liquor space and reduction of cerebral volume	Neuro developmental delay: increased liquor space and reduction of cerebral volume	Deafness, agenesis of choleovestibular nerves, cerebral MRI without further pathologic findings	NA	NA

BM, Bone marrow; *dPmax*, left ventricular contractility index; *HAM test*, acid hemolysin test; *Hb*, hemoglobin; *IVIG*, intravenous immunoglobulin; *IBMF*, inherited bone marrow failure; *LRS*, left to right shunt; *MRI*, magnetic resonance imaging; *NA*, not applicable; *ND*, not determined; *PFO*, patent foramen ovale.

\*World Health Organization percentile calculator at <http://www.infantchart.com>.

†Not specified.

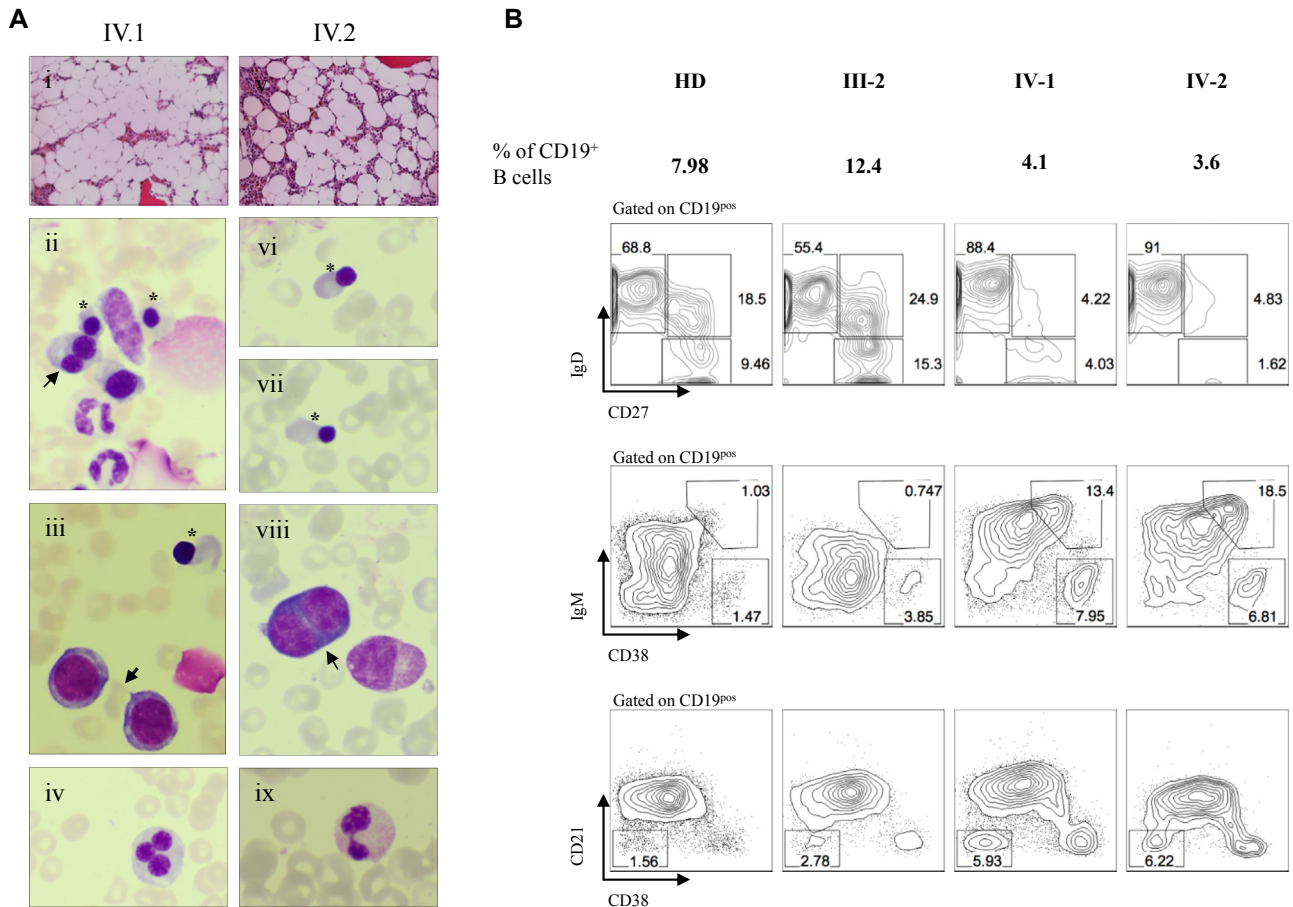


**FIG 2.** Cytohistopathological analysis of bone marrow (BM) samples. **A**, Histopathological analyses of BM biopsy specimens (hematoxylin and eosin staining) depicting hypocellular BM with increase in adipocyte values (Pat IV.1:i and Pat IV.2:vii). Cytological studies of BM aspirates (May-Grunwald-Giemsa) showing myelodysplastic features with binucleated and trinucleated erythroblasts (ii [arrow] and iv) and proerythroblast (viii [arrow]), ectopic nuclear morphology of erythroblasts (ii, iii, vi, and vii [all asterisks]), cytoplasm bridge between proerythroblasts (iii [arrow]), and pseudo-Pelger-Huet anomaly (ix). **B**, Immune phenotype of peripheral blood cells in MYSM1-deficient patients compared with a healthy donor and a parent (III-2).

provided inconsistent results. At several time points, patients were slightly lymphopenic, with decreased absolute numbers of CD4<sup>+</sup> or CD8<sup>+</sup> T cells, but at other time points, relative and absolute numbers of T cells were normal (see Fig E4 and Table E3 in this article's Online Repository at [www.jacionline.org](http://www.jacionline.org)). Proliferation studies of B and T cells did not reveal any significant alterations compared with reference values of healthy age-matched children (see Table E3).

Comprehensive immunohematologic findings of all MYSM1-deficient patients are listed in Table E3.

### Identification of mutations in MYSM1

To investigate the underlying genetic alteration, we performed whole-exome sequencing in patients and their parents according to previously described protocols.<sup>8</sup> On variant filtering, we identified 9 potentially disease-causing variants (see Table E1). Of note, we found a variant in *MYSM1* (NM\_001085487: c.1168G>T: p.E390\*) in a large homozygous interval. The sequence variant c.1168G>T could be confirmed by Sanger sequencing and segregated with the disease phenotype in an autosomal recessive inheritance pattern (Fig 3, A).

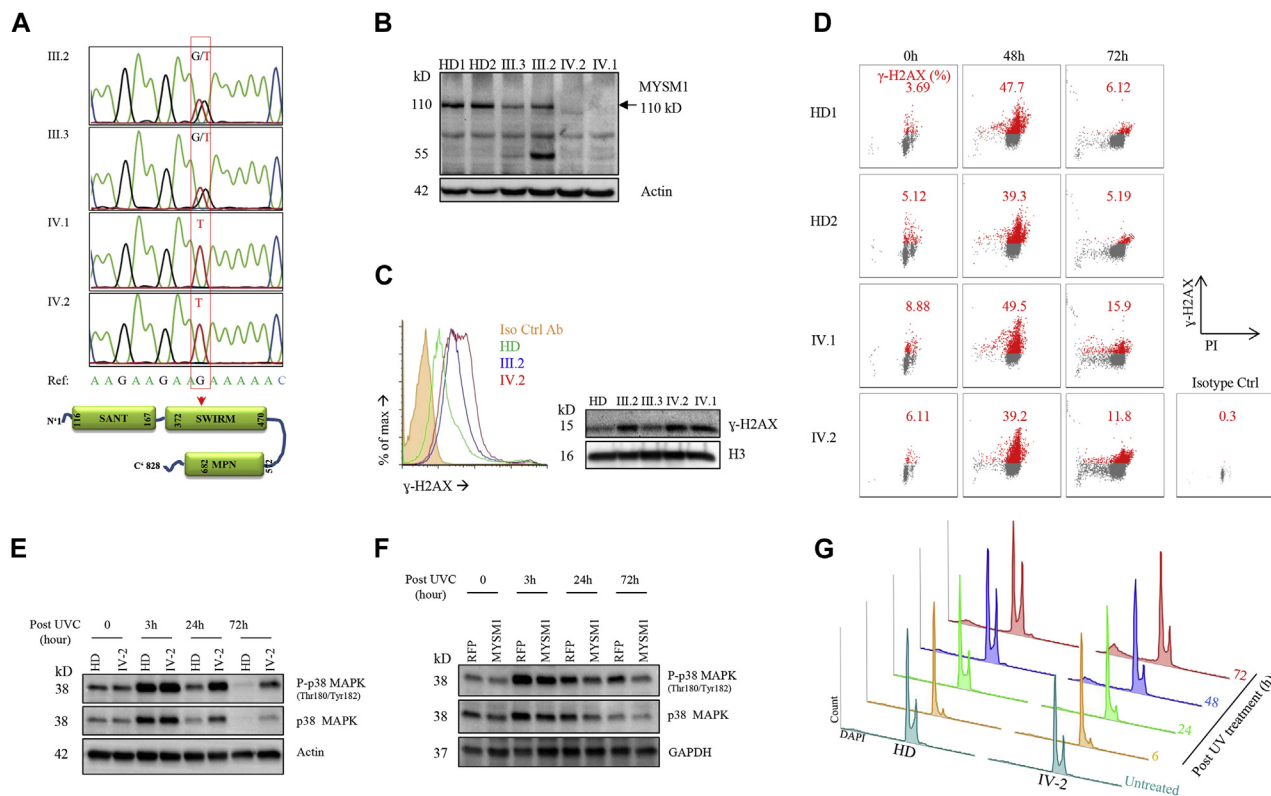


**FIG 3.** Mutation analysis and increased genotoxicity. **A**, Segregation of *MYSM1* mutation in the family. **B**, Western blot (WB) analysis of *MYSM1* protein expression in EBV-LCLs of *MYSM1*-deficient patients compared with that seen in the heterozygous cells of their parents and 2 healthy control subjects (representative data of 3 independent experiments). **C**, Flow cytometry and WB detection of  $\gamma$ -H2AX in EBV-LCLs of an *MYSM1*-deficient patient in comparison with a parent (heterozygous for the mutation) and a healthy control subject (representative data of 3 independent experiments). **D**, Flow cytometric analysis of  $\gamma$ -H2AX levels in PBMCs of *MYSM1*-deficient patients compared with healthy control subjects before and after UV-induced DNA damage induction ( $50 \text{ J/m}^2$ , representative data of 3 independent experiments). **E**, WB analysis of p38 MAPK and phospho-p38 (Thr180/Tyr182) MAPK expression in primary fibroblasts of *MYSM1*-deficient patients and healthy control subjects in response to genotoxic stress (UV irradiation,  $50 \text{ J/m}^2$ ; representative data of 2 independent experiments). **F**, Reconstitution analysis of p38 MAPK activation (phospho-p38, Thr180/Tyr182) in patient IV-2's primary fibroblast transduced by bicistronic lentiviruses expressing *MYSM1*-RFP or RFP only. After transduction, RFP-expressing cells were sorted and irradiated by UVC, and phospho-p38 and total p38 MAPK (Thr180/Tyr182) expression was analyzed by using WB (representative data of 3 independent experiments). The same results were observed on patient IV-1's *MYSM1*-corrected fibroblasts. **G**, Representative experiment of 3 independent flow cytometry-based cell-cycle analyses of *MYSM1*-deficient fibroblasts from a patient and a healthy control subject after UV irradiation-induced DNA damage ( $50 \text{ J/m}^2$ ).

To study the consequences of this mutation leading to a premature stop codon in exon 9 (SWIRM domain), we generated anti-*MYSM1* mAbs. As shown in Fig 3, B, *MYSM1* could not be detected at the expected size in EBV-LCLs generated from the patients, whereas a 110-kDa band representing wild-type *MYSM1* was seen in cells from parents.

### Increased genotoxic stress in *MYSM1*-deficient cells

Murine *Mysm1* deficiency results in increased genomic instability in blood cells.<sup>11,12</sup> Therefore we were interested to see whether *MYSM1*-deficient human patients had similar aberrations. We measured levels of phospho-histone H2AX ( $\gamma$ -H2AX) as a marker for DNA damage in PBMCs and EBV-LCLs. In *MYSM1*-deficient cells from patients, baseline levels of  $\gamma$ -H2AX were increased in comparison with those of

heterozygous parents and healthy donors (HDs) (Fig 3, C and D, and see Fig E5 in this article's Online Repository at [www.jacionline.org](http://www.jacionline.org)). Upon UV irradiation-induced DNA damage,  $\gamma$ -H2AX levels were upregulated independent of *MYSM1* expression. In contrast to control cells, however, patients' cells had a slower decay rate and expressed high  $\gamma$ -H2AX levels, even after 72 hours (Fig 3, D).

The hematopoietic phenotype in *Mysm1*-deficient mice can be reverted by ablation of p53.<sup>12,13</sup> Because p53 is linked to mitogen-activated protein kinase (MAPK) signaling,<sup>14</sup> we next hypothesized that increased cellular stress and genotoxicity in the setting of *MYSM1* deficiency can be associated with increased activation of p38. We induced genotoxic stress in primary fibroblasts by means of UV irradiation and determined expression levels of phosphorylated p38 using Western blotting. Both *MYSM1*-deficient and control cells exhibited increased expression of p38

and phosphorylated p38 in response to UV exposure. In contrast to HD cells, MYSM1-deficient cells had delayed re-equilibration of these stress-associated marks after 24 and 72 hours (Fig 3, E). Moreover, MYSM1-deficient fibroblasts showed increased reactive oxygen species (ROS) production on UV treatment in comparison with control fibroblasts (see Fig E6 in this article's Online Repository at [www.jacionline.org](http://www.jacionline.org)).

To unequivocally prove that the increased susceptibility to genotoxic stress is caused by MYSM1 deficiency, we aimed to reconstitute the cellular phenotype using retrovirus-mediated *MYSM1* gene transfer. We cloned human *MYSM1* in a bicistronic vector expressing red fluorescent protein (RFP) as a reporter gene and transduced fibroblasts from control subjects and patients. As shown in Fig 3, F, and Fig E7 in this article's Online Repository at [www.jacionline.org](http://www.jacionline.org), (partial) protection against the damaging effects induced by UV light, as seen by a more rapid decrease of phosphorylated p38 MAPK, was observed after MYSM1 transduction, whereas transduction of the control vector expressing RFP only had no effect.

In view of a putative role of MYSM1 in DNA-damage checkpoint control,<sup>15</sup> we next analyzed cell-cycle progression and the rate of apoptosis in MYSM1-deficient human fibroblast cells. Six hours after UV irradiation, we observed an arrest in the G1 phase and a reduced number of cells in the G2-M phase in all cells independent of MYSM1 expression. HD cells re-equilibrated their regular distribution of cell-cycle phases, whereas MYSM1-deficient cells showed prolonged G1 arrest and a slower recovery (G2/M: 32.8% and 16.5%, respectively). The percentage of apoptotic cells (sub-G1) was increased in cells from patients in contrast to the percentage in cells from HDs (27.8% vs 11.9%; Fig 3, G). In line with these data, MYSM1-deficient EBV-LCLs also had increased sensitivity to etoposide-induced apoptosis when compared with heterozygous parent or HD cells (see Fig E8 in this article's Online Repository at [www.jacionline.org](http://www.jacionline.org)).

Finally, we asked whether increased UV-induced genotoxic stress would lead to decreased clonogenic survival of fibroblasts. We plated 100 to 4000 cells followed by UV exposure and enumerated surviving cell clones after 20 days. MYSM1-deficient fibroblasts had reduced clonogenic growth when compared with cells from HDs (see Fig E9 in this article's Online Repository at [www.jacionline.org](http://www.jacionline.org)).

### Allogeneic hematopoietic stem cell transplantation

In view of progressive BMF with trilineage cytopenia, both patients underwent allogeneic hematopoietic stem cell transplantation (HSCT) from HLA-matched adult family donors at the age of 42 and 23 months, respectively (see Fig E3). The reduced-intensity conditioning regimen<sup>16</sup> included fludarabine (150 mg/m<sup>2</sup>), treosulfan (42 g/m<sup>2</sup>), and alemtuzumab (0.4 mg/kg). Graft-versus-host disease prophylaxis included cyclosporine and mycophenolate mofetil. The early posttransplantation course was uneventful in both patients. Two years after transplantation, they are full donor chimeras with normal peripheral blood counts and without signs of graft-versus-host disease (see Fig E3). In patient IV-1 1 year after transplantation, hyperthyroidism (Graves-Basedow disease) has been diagnosed, probably reflecting a complication after transplantation. In patient IV-2 cardiomyopathy, which is currently treated with captopril, and neurological development show a favorable course.

### DISCUSSION

We here report on clinical, immunologic, and molecular features in 2 siblings with MYSM1 deficiency. MYSM1 was originally discovered as a member of the histone H2A deubiquitinase complex coordinating histone acetylation and H1 dissociation in transcriptional regulation.<sup>2</sup> Subsequent studies in *Mysm1*-deficient mice have revealed that *Mysm1* plays a critical role in B-cell maturation through derepression of transcription of early B-cell factor 1 (*Ebf1*), paired box 5 (*Pax5*), and other B-lymphoid genes.<sup>3</sup> Jiang et al<sup>3</sup> suggested that MYSM1 mechanistically antagonizes action of the polycomb repressive complex 1 (PRC1) on the *EBF1* promoter region, resulting in activation of transcription factor *E2- $\alpha$*  and *PAX5*.<sup>3</sup> In line with mouse data, we here report human MYSM1 deficiency causes BMF associated with B-cell deficiency. B-cell defect in MYSM1 deficiency has also recently been reported by 2 other groups.<sup>6,7</sup>

Further investigations of *Mysm1*-deficient mice disclosed that the epigenetic regulatory function of *Mysm1* is not restricted to B cells but might also affect other immune and nonimmune cells.<sup>5,17-20</sup> Moreover, Panda et al<sup>21</sup> reported that MYSM1, beyond its crucial role in the nucleus, can function in the cytoplasm as a deubiquitinating enzyme regulating innate immunity responses. In line with these data, we also observed impaired vaccination and antibody titers, but in contrast, T-cell immunity was not affected in our patients.

DNA damage triggers cellular repair activities associated with accumulation of ubiquitin-H2A at  $\gamma$ -H2AX containing foci.<sup>22,23</sup> Upon successful completion of DNA repair, dephosphorylation and removal of  $\gamma$ -H2AX and ubiquitin-H2A are essential for resuming coordinated progression of the cell cycle.<sup>24,25</sup>

Deubiquitinating enzymes, such as ubiquitin-specific peptidase 3 (*Usp3*) and *Usp16*, might regulate the cellular response toward DNA damage.<sup>26-28</sup> Our data show that in the absence of MYSM1, the cellular re-equilibration of cell-cycle progression is perturbed, suggesting that MYSM1 is involved in DNA damage-induced repair.

Cross-activation of p38 and p53 has been shown to play a key role in stress responses, in particular after genotoxic stress.<sup>14,29-31</sup> When Nijnik et al<sup>11</sup> discovered increased levels of  $\gamma$ -H2AX, ROS, and p53 in *Mysm1*-deficient murine hematopoietic cells, they hypothesized a critical role for p53 linked to *Mysm1*. In fact, the generation of *Mysm1*<sup>-/-</sup>*p53*<sup>-/-</sup> double-deficient mice confirmed this idea because the hematopoietic defects observed in *Mysm1*-deficient mice were completely reversed in the absence of p53.<sup>12,13</sup> Subsequent studies have recently shown that p53 and *Mysm1* colocalize to genomic loci known to be transcriptionally controlled by p53,<sup>32</sup> suggesting that *Mysm1* controls accessibility of defined genomic loci to transcription factors. However, the exact sequence of events remains to be elucidated. Our data show that MYSM1-deficient cells are characterized by a state of increased stress (evidence by phosphorylation of p38) and delayed return to a coordinated cell-cycle progression. We assume that these effects are linked to both altered histone deubiquitination and imbalanced transcriptional regulation, but at this point, we cannot yet define the molecular steps in greater detail.

Two previous reports of patients with MYSM1 deficiency have implicated its importance in adequate hematopoiesis and B-cell development.<sup>6,7</sup> We expand on these observations and show that MYSM1 deficiency is associated with developmental aberrations, myelodysplastic features, and increased susceptibility to

genotoxic stress. We also document that the hematopoietic defects in patients with MYSM1 deficiency can be cured by allogeneic HSCT. Conditioning regimens for allogeneic HSC transplants must be carefully selected in patients with increased susceptibility to genotoxicity, such as Fanconi anemia and Nijmegen breakage syndrome. Our regimen based on fludarabine and treosulfan appeared to be safe and effective for stable engraftment of allogeneic stem cells without undue toxicity.

In summary, our results expand the spectrum of rare BMF syndromes associated with immunodeficiency and developmental aberrations.

We thank the family for participating in this study and the medical and nursing staff for excellent clinical care. We dedicate this work to Dr Jacek Puchalka, who died in a tragic accident in the Bavarian Alps while these investigations were ongoing.

#### Key messages

- MYSM1 deficiency causes B-cell immunodeficiency associated with complex developmental aberrations and inherited BMF syndrome.
- MYSM1 controls genotoxic stress responses.
- The immunologic and hematologic aberrations in patients with MYSM1 deficiency can be cured by using allogeneic HSCT.

#### REFERENCES

1. Shimamura A, Alter BP. Pathophysiology and management of inherited bone marrow failure syndromes. *Blood Rev* 2010;24:101-22.
2. Zhu P, Zhou WL, Wang JX, Puc J, Ohgi KA, Erdjument-Bromage H, et al. A histone H2A deubiquitinase complex coordinating histone acetylation and H1 dissociation in transcriptional regulation. *Mol Cell* 2007;27:609-21.
3. Jiang XX, Nguyen Q, Chou YC, Wang T, Nandakumar V, Yates P, et al. Control of B cell development by the histone H2A deubiquitinase MYSM1. *Immunity* 2011;35:883-96.
4. Wang T, Nandakumar V, Jiang XX, Jones L, Yang AG, Huang XF, et al. The control of hematopoietic stem cell maintenance, self-renewal, and differentiation by Mym1-mediated epigenetic regulation. *Blood* 2013;122:2812-22.
5. Nandakumar V, Chou YC, Zang LD, Huang XF, Chen SY. Epigenetic control of natural killer cell maturation by histone H2A deubiquitinase, MYSM1. *Proc Natl Acad Sci U S A* 2013;110:E3927-36.
6. Alsultan A, Shamseldin HE, Osman ME, Aljabri M, Alkuraya FS. MYSM1 is mutated in a family with transient transfusion-dependent anemia, mild thrombocytopenia, and low NK- and B-cell counts. *Blood* 2013;122:3844-5.
7. Le Guen T, Touzot F, Andre-Schmutz I, Lagresle-Peyrou C, France B, Kermasson L, et al. An in vivo genetic reversion highlights the crucial role of Myb-Like, SWIRM, and MPN domains 1 (MYSM1) in human hematopoiesis and lymphocyte differentiation. *J Allergy Clin Immunol* 2015;136:1619-26, e1-5.
8. Triot A, Jarvinen PM, Arostegui JI, Murugan D, Kohistani N, Dapena Diaz JL, et al. Inherited biallelic CSF3R mutations in severe congenital neutropenia. *Blood* 2014;123:3811-7.
9. Piatosa B, Wolska-Kusnierz B, Pac M, Siewiera K, Galkowska E, Bernatowska E. B cell subsets in healthy children: reference values for evaluation of B cell maturation process in peripheral blood. *Cytometry B Clin Cytom* 2010;78:372-81.
10. Morbach H, Eichhorn EM, Liese JG, Girschick HJ. Reference values for B cell subpopulations from infancy to adulthood. *Clin Exp Immunol* 2010;162:271-9.
11. Nijnik A, Clare S, Hale C, Raisen C, McIntyre RE, Yusa K, et al. The critical role of histone H2A-deubiquitinase Mym1 in hematopoiesis and lymphocyte differentiation. *Blood* 2012;119:1370-9.
12. Gatzka M, Tasdogan A, Hainzl A, Allies G, Maity P, Wilms C, et al. Interplay of H2A deubiquitinase 2A-DUB/Mym1 and the p19(ARF)/p53 axis in hematopoiesis, early T-cell development and tissue differentiation. *Cell Death Differ* 2015;22:1451-62.
13. Belle JI, Langlais D, Petrov JC, Pardo M, Jones RG, Gros P, et al. p53 mediates loss of hematopoietic stem cell function and lymphopenia in Mym1 deficiency. *Blood* 2015;125:2344-8.
14. Gong XW, Liu AH, Ming XY, Deng P, Jiang Y. UV-induced interaction between p38 MAPK and p53 serves as a molecular switch in determining cell fate. *FEBS Lett* 2010;584:4711-6.
15. Nishi R, Wijnhoven P, le Sage C, Tjeertes J, Galanty Y, Forment JV, et al. Systematic characterization of deubiquitylating enzymes for roles in maintaining genome integrity. *Nat Cell Biol* 2014;16:1016-26.
16. Myers KC, Howell JC, Wallace G, Dandoy C, El-Bietar J, Lane A, et al. Poor growth, thyroid dysfunction and vitamin D deficiency remain prevalent despite reduced intensity chemotherapy for hematopoietic stem cell transplantation in children and young adults. *Bone Marrow Transplant* 2016;51:980-4.
17. Won H, Nandakumar V, Yates P, Sanchez S, Jones L, Huang XF, et al. Epigenetic control of dendritic cell development and fate determination of common myeloid progenitor by Mym1. *Blood* 2014;124:2647-56.
18. Jiang XX, Chou Y, Jones L, Wang T, Sanchez S, Huang XF, et al. Epigenetic regulation of antibody responses by the histone H2A deubiquitinase MYSM1. *Sci Rep* 2015;5:13755.
19. Huang XF, Nandakumar V, Tumurkhuu G, Wang T, Jiang X, Hong B, et al. Mym1 is required for interferon regulatory factor expression in maintaining HSC quiescence and thymocyte development. *Cell Death Dis* 2016;7:e2260.
20. Li P, Yang YM, Sanchez S, Cui DC, Dang RJ, Wang XY, et al. Deubiquitinase MYSM1 is essential for normal bone formation and mesenchymal stem cell differentiation. *Sci Rep* 2016;6:22211.
21. Panda S, Nilsson JA, Gekara NO. Deubiquitinase MYSM1 regulates innate immunity through inactivation of TRAF3 and TRAF6 complexes. *Immunity* 2015;43:647-59.
22. Huen MS, Grant R, Manke I, Minn K, Yu X, Yaffe MB, et al. RNF8 transduces the DNA-damage signal via histone ubiquitylation and checkpoint protein assembly. *Cell* 2007;131:901-14.
23. Mailand N, Bekker-Jensen S, Fastrup H, Melander F, Bartek J, Lukas C, et al. RNF8 ubiquitylates histones at DNA double-strand breaks and promotes assembly of repair proteins. *Cell* 2007;131:887-900.
24. Keogh MC, Kim JA, Downey M, Fillingham J, Chowdhury D, Harrison JC, et al. A phosphatase complex that dephosphorylates gammaH2AX regulates DNA damage checkpoint recovery. *Nature* 2006;439:497-501.
25. Chowdhury D, Keogh MC, Ishii H, Peterson CL, Buratowski S, Lieberman J. gamma-H2AX dephosphorylation by protein phosphatase 2A facilitates DNA double-strand break repair. *Mol Cell* 2005;20:801-9.
26. Lancini C, van den Berk PC, Vissers JH, Gargiulo G, Song JY, Hulsman D, et al. Tight regulation of ubiquitin-mediated DNA damage response by USP3 preserves the functional integrity of hematopoietic stem cells. *J Exp Med* 2014;211:1759-77.
27. Nicassio F, Corrado N, Vissers JH, Areces LB, Bergink S, Martejn JA, et al. Human USP3 is a chromatin modifier required for S phase progression and genome stability. *Curr Biol* 2007;17:1972-7.
28. Shanbhag NM, Rafalska-Metcalf IU, Balane-Bolivar C, Janicki SM, Greenberg RA. ATM-dependent chromatin changes silence transcription in cis to DNA double-strand breaks. *Cell* 2010;141:970-81.
29. She QB, Chen N, Dong Z. ERKs and p38 kinase phosphorylate p53 protein at serine 15 in response to UV radiation. *J Biol Chem* 2000;275:20444-9.
30. Bulavin DV, Saito S, Hollander MC, Sakaguchi K, Anderson CW, Appella E, et al. Phosphorylation of human p53 by p38 kinase coordinates N-terminal phosphorylation and apoptosis in response to UV radiation. *EMBO J* 1999;18:6845-54.
31. Huang C, Ma WY, Maxiner A, Sun Y, Dong Z. p38 kinase mediates UV-induced phosphorylation of p53 protein at serine 389. *J Biol Chem* 1999;274:12229-35.
32. Belle JI, Petrov JC, Langlais D, Robert F, Cencic R, Shen S, et al. Repression of p53-target gene Bbc3/PUMA by MYSM1 is essential for the survival of hematopoietic multipotent progenitors and contributes to stem cell maintenance. *Cell Death Differ* 2016;23:759-75.